



Around the thermodynamic limitations of supercapacitors operating in aqueous electrolytes



Krzysztof Fic^{1,*}, Mikolaj Meller, Jakub Menzel¹, Elzbieta Frackowiak¹

Poznan University of Technology, Institute of Chemistry and Technical Electrochemistry, Berdychowo 4, 60965 Poznan, Poland

ARTICLE INFO

Article history:

Received 6 November 2015
Received in revised form 10 February 2016
Accepted 13 February 2016
Available online 16 February 2016

Keywords:

hybrid electrolytes
aqueous medium
high voltage capacitors
mixed electrolytes

ABSTRACT

This paper reports on a primary study of the capacitor system that can successfully overcome the main drawback of aqueous electrolytes, i.e. low max. voltage and then low energy density of the device. Our idea employs hybridization of electrolytes, i.e. use of two separated electrolytes with different pH values, each for one electrode. In such a way, the capacitor voltage is extended to 2.1 V. 6 mol L⁻¹ KOH plays the role of electrolyte for the negative electrode whereas 1 mol L⁻¹ H₂SO₄ or 5 mol L⁻¹ LiNO₃ are electrolytic solutions for a positive one. This idea allows us to take advantage of very negative hydrogen evolution potential for KOH and high overpotential of oxygen evolution, especially for LiNO₃ solutions. Accordingly, it was possible to maintain almost 100 F g⁻¹ after 25 000 cycles at 1 A g⁻¹, gaining the energy more than 10 Wh kg⁻¹ along the average power of 1 kW kg⁻¹.

© 2016 Elsevier Ltd. All rights reserved.

1. Introduction

Modern supercapacitors serve as excellent power sources providing demanded energy in a very short time [1]. However, their wide application is so far limited by rather moderate energy density. Hence, a lot of research in the supercapacitors field concerns an improvement of that feature. Since the energy delivered by electrochemical capacitor depends on capacitance value and squared operating voltage, a general outline for such a research starts reasonably with capacitance enhancement or employment of the electrolyte with wide electrochemical window.

Several approaches have been implemented to date aiming to increase the capacitance value of the electrodes. As the capacitance of electrical double layer is limited by properties of an electrode material such as porosity and surface functionality [2–4] and at the same time related particularly to non-adjustable ion size [5,6], activated carbons with well-developed microporosity are recently the most often applied materials for this application [7]. Although several advanced materials like templated carbons [8,9], carbide-derived carbons [10,11], carbon nanotubes [12] or MXenes [13,14], characterized by tuneable properties, high capacitance values and excellent charge propagation have already been proposed, it seems that the material limit in terms of the interface accessible for ions is already reached [15–17]. On the other hand, electrostatic double-

layer charging may, however, be accompanied by pseudocapacitance effects with the faradaic origin and then the capacitance values may be improved by incorporation of redox reactions. This phenomenon has been discussed widely elsewhere [18], especially for electrodes composed of transition metal oxides like MnO₂ [19,20] or for several electrolytic solutions demonstrating redox activity and preserving a superior capacitive performance [21–23]. However, it has to be noticed that enhancement of capacitance value by pseudocapacitive effects is always a compromise between high power and high energy density [24].

The maximum voltage of the capacitor mainly depends on the electrolyte used. Application of organic electrolytes (including ionic liquids) allows the voltage of 3.2 V to be reached [25–27], thus, energy density might be improved remarkably. Notwithstanding, despite several advantages of ionic liquids (wide electrochemical stability, negligible vapour pressures, limited flammability), their application in supercapacitors is affected by low conductivity which aggravates the power response. Obviously, for application requiring moderate power, they still seem to be an optimal choice.

Supercapacitors operating in organic electrolytes based on propylene carbonate or acetonitrile solutions demonstrate the maximum stability of ca. 2.7 V but flammability, safety and several environmental aspects are in this case of the major concern. However, it has to be noticed that electrochemical capacitors operating with organic electrolytes are at the moment the commercial products offered by the market.

On the other hand, water-based electrolytes offer high conductivity (i.e. power rates), safe operation even at elevated

* Corresponding author. Tel.: +48 61 665 32 38; fax: +48 61 665 37 91.
E-mail address: Krzysztof.Fic@put.poznan.pl (K. Fic).

¹ ISE member.

temperatures and stable cycle performance. Unfortunately, the electrochemical stability of water electrolytes is limited by water decomposition at 1.23 V. Hence, aqueous-based devices demonstrate moderate energy density. Additionally, the maximum voltage for H_2SO_4 or KOH electrolytes is very often limited to only 0.8–1.0 V [28,29] because of overpotentials for hydrogen/oxygen evolution and carbon electrode ‘corrosion’ which might aggravate the cyclability and efficiency. Technological aspects related to current collector corrosion in the aqueous environment might, however, be solved by corrosion inhibitors dissolved in electrolytes, which furthermore can enhance the capacitance values by pseudocapacitance effects [30].

Fortunately, the low voltage value of aqueous-based supercapacitor can be improved by electrode mass balancing [16,17,31–33] or by tailoring carbon properties for the positive and negative electrode, which enables even 2.0 V to be reached [34,35]. Adjustment of the electrode masses allows the operating potential of the electrodes to be maintained within optimal range and evolution of either H_2 or O_2 to be avoided [32,33]. Another way that allows theoretical limits to be overcome is the application of pH-neutral electrolytic solutions of inorganic salts such as Li_2SO_4 [36], Na_2SO_4 [37] and K_2SO_4 [38,39]. To date, the most promising performance was reported for Li_2SO_4 solutions [36,40]. However, one should be aware, that the possibility of voltage extension for devices operating in these electrolytes strongly depends on the electrode material, binder [41] and current collector used; hydrogen storage contribution in microporous carbons [40], ion/solvent and ion/pore interactions [36], as well as current collector corrosion effects, have to be considered at a first glance. Despite all these technological concerns, aqueous solutions seem to be the best choice if the high power density, user safety and long term operation features are required.

In this paper, we propose a different method for the capacitor voltage/energy enhancement. Since the hydrogen and oxygen evolution potentials are pH dependent, thus, applying an electrolyte with pH lower than 7 as an electrolytic medium for the positive electrode and an electrolyte with pH higher than 7 for the negative electrode, it is possible to ‘spread’ the overpotentials of oxygen and hydrogen evolution.

In order to enhance the voltage window of water-based electrochemical capacitors, we combine two well-characterized aqueous electrolytes in one system to take advantages of each of them. By using 1 mol L^{-1} H_2SO_4 or 5 mol L^{-1} LiNO_3 as an electrolyte for the positive electrode and 6 mol L^{-1} KOH for the negative one, we have obtained better performance than using a single electrolyte. This kind of capacitor works at the voltage as high as 2.1 V and demonstrates competitive power/energy performance.

2. Experimental

For electrochemical investigations, several aqueous solutions were prepared in various concentrations, i.e. 1 mol L^{-1} H_2SO_4 , 6 mol L^{-1} KOH and 5 mol L^{-1} LiNO_3 . Activated carbon powder (AAC) was used as an electrode material; physicochemical characteristic details of this material can be found elsewhere [42,43]. For this study, the electrodes were prepared in the form of pellets (0.785 cm^2) that consisted of 85 wt.% of activated carbon, 10 wt.% of PTFE binder and 5 wt.% of carbon black. Additionally, in order to eliminate the influence of binder, for cyclic voltammetry and galvanostatic cycling measurements, a binder-free carbon tissue was used (Kynol ACC 507–20). It has to be noted here that both carbons demonstrate a very similar specific surface area (1865 $\text{m}^2 \text{g}^{-1}$ for tissue and 1901 $\text{m}^2 \text{g}^{-1}$ for powder), microporous character (from 2D NL-DFT calculations [44,45]) and oxygen content less than 5% wt. The mass of each pellet was about 8 mg. All

Table 1
Electrolyte.

	Theoretical pH	E_{H_2} vs. SHE [V]	E_{O_2} vs. SHE [V]
1 mol L^{-1} H_2SO_4	0	−0.018	1.230
6 mol L^{-1} KOH	14	−0.872	0.358
5 mol L^{-1} LiNO_3	7	−0.413	0.817

capacitance values were calculated per active mass of one electrode, if not stated otherwise.

Experiments were carried out in a two- and three-electrode cell (Swagelok[®] system) and investigated by cyclic voltammetry (1–50 mV s^{-1}), constant current charging/discharging (0.2–20 A g^{-1}) and electrochemical impedance spectroscopy (100 kHz–1 mHz, ± 10 mV voltage amplitude), using VMP3/Z BioLogic multichannel potentiostat/galvanostat. pH has been measured using flat-membrane electrode combined with 848 Titrino plus[®] compact titrator (Metrohm, Switzerland). For three-electrodes investigations, three different reference electrodes were used: $\text{Hg}|\text{HgO}$ for alkaline medium, $\text{Hg}|\text{Hg}_2\text{SO}_4$ for acidic one and saturated calomel electrode for a neutral solution. All potential values measured have been recalculated with respect to Normal Hydrogen Electrode for convenient comparison.

Capacitors were assembled in different electrolyte combinations, i.e.: a) 1 mol L^{-1} H_2SO_4 for the positive electrode and 6 mol L^{-1} KOH for the negative electrode; b) 5 mol L^{-1} LiNO_3 (positive electrode) and 6 mol L^{-1} KOH (negative electrode). It has to be noticed that electrodes were soaked in a small amount of electrolyte (ca. 100 μL) without any excess of it. In order to avoid their mixing and transport through the membrane (significant pH and concentration gradient), a commercially available micro-glass fibre filter (Munktell MGC) immersed in 5 mol L^{-1} LiNO_3 aqueous and buffer solutions were used for separation. The separators were soaked in respective solutions for 1 hour without any further treatment. The excess of the solution has been removed, but the sponge-like structure of the separator served as an electrolyte reservoir. Moreover, the ‘electrode’ solutions have been contacted with the neutral solution, hence, firstly they were neutralized or diluted in the separator. Since the electrodes are separated by neutral solution and there was no excess of it, we assume that local pH change in the bulk of the electrode is negligible (but slight dilution cannot be excluded at the separator/electrode interface). At the same time, we preserved a high ionic conductivity in the separator (by 5 mol L^{-1} LiNO_3 solution), thus, an internal resistance did not increase.

3. Results and discussion

Considering potentials of H_2 and O_2 evolution in both media (Table 1) one can observe interesting characteristics which might be successfully used for cell voltage enhancement.

The most negative potential of hydrogen evolution is maintained for potassium hydroxide, therefore applying it as an electrolyte for the negative electrode seems to be reasonable.

Indeed, cyclic voltammetry measurements (Fig. 1) confirm that electrode operating in 6 mol L^{-1} KOH can operate in the deep negative potential region. Moreover, theoretical potential of hydrogen evolution (−0.872 V vs. SHE) has been exceeded remarkably up to −1.7 V vs. SHE, but electrolyte decomposition was not observed; a significant increase of current recorded is attributed to reversible hydrogen electrosorption in carbon material during negative polarisation, followed by its oxidation during positive polarisation. It has to be noticed that electrode capacity within the EDL range is of 25 mAh g^{-1} (i.e. capacitance of ca. 180 F g^{-1} within 0.5 V potential range) whereas for extended window with significant contribution from pseudocapacitive

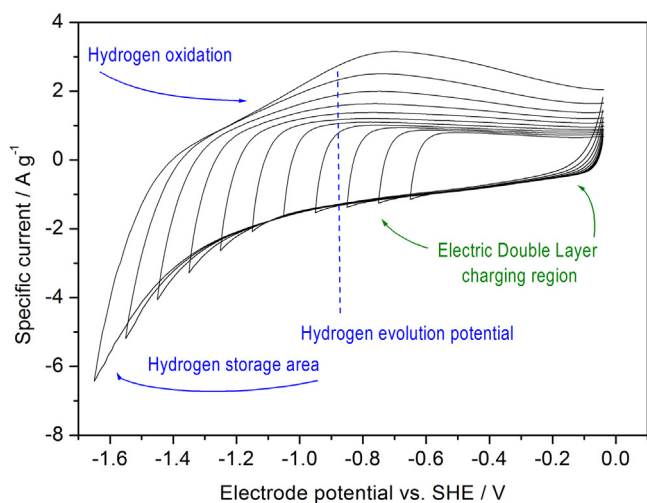


Fig. 1. Cyclic voltammograms (5 mV s^{-1}) for AC electrode operating in 6 mol L^{-1} KOH solution; three-electrode cell configuration, ACC 507-20 activated carbon tissue as working and counter electrode material, Hg/HgO in 6 mol L^{-1} KOH as a reference one.

hydrogen storage the electrode capacity is of 160 mAh g^{-1} (i.e. capacitance of 360 F/g in 1.6 V potential range). This double increase of capacitance value is a positive effect unless the reasonable reversibility of hydrogen storage/oxidation process is maintained; it has to be noticed, that in parallel to hydrogen storage in carbon, its recombination and evolution may occur and then aggravate the efficiency and long-term performance.

In order to match a suitable electrolyte for the positive electrode one have to consider the electrolyte with high stability at oxidative conditions: either sulphuric acid solution with the highest oxygen evolution potential (i.e. $+1.23 \text{ V}$ vs. SHE) or lithium nitrate solution with slightly lower oxygen evolution potential (i.e. $+0.817 \text{ V}$ vs. SHE) but with stabilizing effect of solvated Li^+ against oxidation.

Such a conjunction gives the following options:

(–) 6 mol L^{-1} KOH/ 1 mol L^{-1} H_2SO_4 (+) $E_{\text{cell}} = 2.102 \text{ V}$

(–) 6 mol L^{-1} KOH/ 5 mol L^{-1} LiNO_3 (+) $E_{\text{cell}} = 1.689 \text{ V}$

In order to determine the electrochemical behaviour of carbon electrodes operating both in 1 mol L^{-1} H_2SO_4 and 5 mol L^{-1} LiNO_3 , cyclic voltammetry at 5 mV s^{-1} have been performed in the conventional three-electrode cell.

As expected, the electrochemical behaviour of AC electrode in the acidic electrolyte (Fig. 2) is significantly different than in alkaline solution. One may observe especially a strong redox response from oxygen based-functionalities on the carbon surface, near to $+0.6 \text{ V}$ vs. SHE. This might protect the electrode against further oxidation or oxygen evolution reaction. Hydrogen storage in acidic medium is rather negligible; it can be seen that no hysteresis loop is observed at negative potential values. Moreover, the hydrogen storage contribution to the capacitance value is also rather negligible: the capacity of the electrode within EDL charging/discharging range is 48 mAh g^{-1} (i.e. capacitance of 249 F g^{-1} within 0.7 V potential range), whereas the capacity for entire window (1.5 V) is 110 mAh g^{-1} (capacitance of 264 F g^{-1}). The values of electrode capacitance are remarkably higher than in alkaline medium (28%), but this enhancement originates from the exploitation of oxygen-based functionalities being extremely active in acidic solutions. Finally, it seems that acidic electrolyte could be reasonably considered as a solution for the positive electrode in a hybrid system.

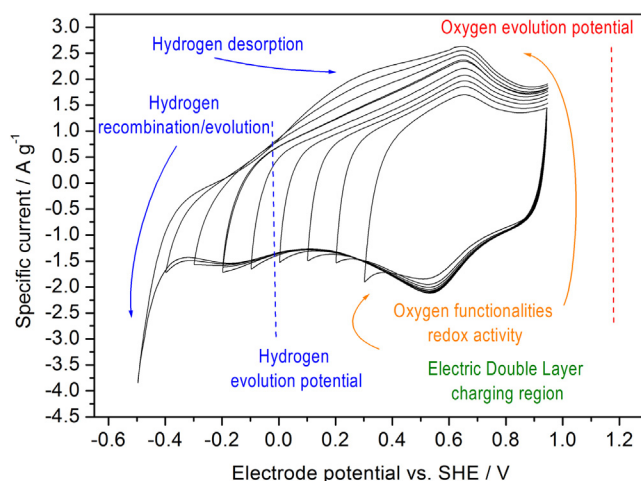


Fig. 2. Cyclic voltammograms (5 mV s^{-1}) for AC electrode operating in 1 mol L^{-1} H_2SO_4 solution; three-electrode cell configuration, ACC 507-20 activated carbon tissue as working and counter electrode material, Hg/Hg $_2\text{SO}_4$ in 1 mol L^{-1} H_2SO_4 as a reference one.

Notwithstanding, use of an acidic electrolyte might arise the question of rapid corrosion and user safety, hence, neutral electrolyte, namely 5 mol L^{-1} LiNO_3 has been also investigated (Fig. 3). The reason for applying this electrolyte was related to the high conductivity (ca. 147 mS cm^{-1}) and high concentration diminishing the gradient if tentatively combined with 6 mol L^{-1} KOH. The difference in the concentrations of ionic species, especially K^+ and Li^+ might provoke undesirable transport of the moieties between electrode and separator components. However, the mobility of Li^+ specimen is significantly lower than K^+ [36]. Moreover, we tended to preserve the same ionic strength throughout the system (and to some extent the osmotic force) in order to avoid the losses in electric potential along the double layer and then, an internal resistance increase.

The electrochemical response of the AC electrode in pH neutral electrolyte solution (pH 7.7) is surprisingly similar to the response in acidic medium. However, the redox response from oxygen-based functionalities is shifted towards more negative values, i.e. $+0.4 \text{ V}$ vs. SHE. Their contribution to total capacitance is enhanced by pseudocapacitance effect from hydrogen storage; for electrical

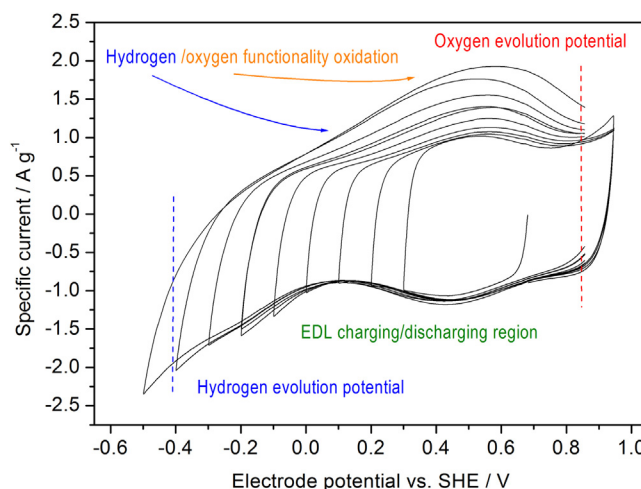


Fig. 3. Cyclic voltammograms (5 mV s^{-1}) for AC electrode operating in 5 mol L^{-1} LiNO_3 solution; three-electrode cell configuration, ACC 507-20 activated carbon tissue as working and counter electrode material, calomel electrode as a reference one.

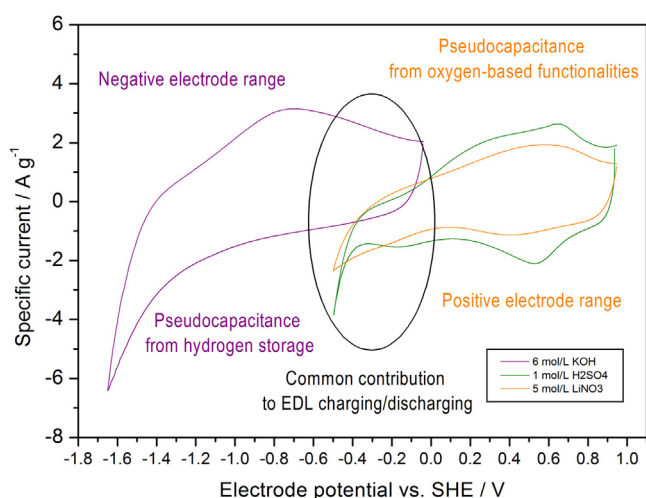


Fig. 4. Comparison of cyclic voltammograms (5 mV s^{-1}) for AC electrodes operating in various electrolyte solutions; three-electrode cell configuration, ACC 507-20 activated carbon tissue as working and counter electrode material.

double layer region (ca. 0.6 V), the capacitance value is of 33 mAh g^{-1} , i.e. 186 F g^{-1} , whereas for extended potential window (ca. 1.4 V) is of 90 mAh g^{-1} , i.e. 232 F g^{-1} . It seems that 20% of capacitance increase might be attributed to reversible hydrogen electrosorption; however, additional slight oxidation of carbon surface in the presence of NO_3^- specimen, contributing to capacitance increase cannot be neglected. Finally, it seems that LiNO_3 electrolytic solution preserves similar condition as acidic one, but its less aggressive character makes this electrolyte more promising for application in a real device.

A quite interesting observation concerns the ‘ion sieving/exchange effect’. In alkaline solution ($6 \text{ mol L}^{-1} \text{ KOH}$), K^+ specimen is preferably adsorbed in micropores of the negative electrode (or during negative polarisation), hence, one might observe a typical capacitive response until hydrogen evolution potential is reached (Fig. 4).

In the case of an acidic or neutral solution, electrodes polarised negatively responded with significant deterioration of capacitive current. Thus, one might conclude that the Point of Zero Charge (pzc) is definitely different, and there is a dramatic imbalance of electrode charging mechanisms. Moreover, the effective radius of potassium in aqueous solution is remarkably smaller than that of

lithium [36]. Hence, potassium ions can easily accommodate in micropores while Li^+ cannot. Accordingly, one should expect lower overpotential of hydrogen evolution/storage in Li^+ containing electrolytes but with remarkably higher potential of its oxidation. This is in good agreement with other reports [37,41].

Aforementioned considerations were based on results obtained in three-electrode configuration. In order to verify the concept proposed, typical two electrode systems were assembled and subjected to similar investigations. At a first glance, cyclic voltammetry technique confirmed the possibility of combining two completely different electrolytes with extremely various pH values. Assembled devices demonstrated satisfying electrochemical response. In Fig. 5 one can observe that $1 \text{ mol L}^{-1} \text{ H}_2\text{SO}_4$ and $6 \text{ mol L}^{-1} \text{ KOH}$ solutions, when applied to single electrolytes for individual electrodes, can provide acceptable capacitance values even at moderate scan rate (10 mV s^{-1}), i.e. 167 and 151 F g^{-1} , respectively. However, their effective electrochemical window is lower than expected according to thermodynamic values, i.e. about $0.8\text{--}1.0 \text{ V}$.

In symmetric systems, the lower voltage is caused by either hydrogen or oxygen evolution which occur with very low overpotentials (essentially in acidic solutions) and provokes precocious water decomposition and performance fade. On the other hand, in the case of acid/alkaline couple, the capacitance value is a little bit lower (143 F g^{-1}) but the electrochemical window is remarkably wider (up to 2 V), and this is a great benefit of the concept and results in energy enhancement. For neutral/alkaline combination, it is worth noting that electrochemical capacitor only with lithium nitrate solution can operate safely with voltage values even up to 1.6 V with average capacitance values of 157 F g^{-1} . However, the capacitance retention during cycles would be aggravated by decomposition products of LiNO_3 electrolyte operating close to the decomposition potentials. Nevertheless, in order to reach 2.1 V , it is still necessary to replace the electrolyte for the negative electrode by potassium hydroxide (Fig. 6).

The three electrode investigation (Fig. 6) shows the interesting behaviour of each electrode; an additional reference electrode introduced to the Swagelok[®] system allows potential ranges of both electrodes to be determined. In the case of LiNO_3/KOH electrolyte couple, one can see that the negative electrode approaches -0.867 V vs. SHE . It means that only ca. 5 mV remains until the theoretical value of hydrogen evolution potential is reached; thus, we did not notice any current response related to electrolyte decomposition. The positive electrode significantly

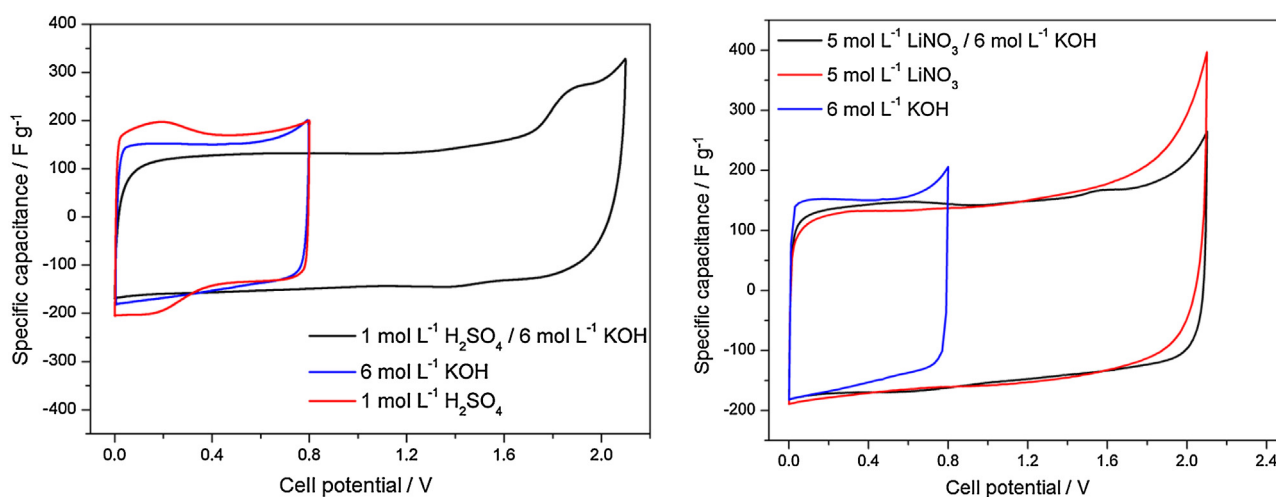


Fig. 5. Cyclic voltammograms for capacitors operating in different couples of electrolytes and appropriate single components at 10 mV s^{-1} scan rate: A) acid-alkaline and B) neutral-alkaline.

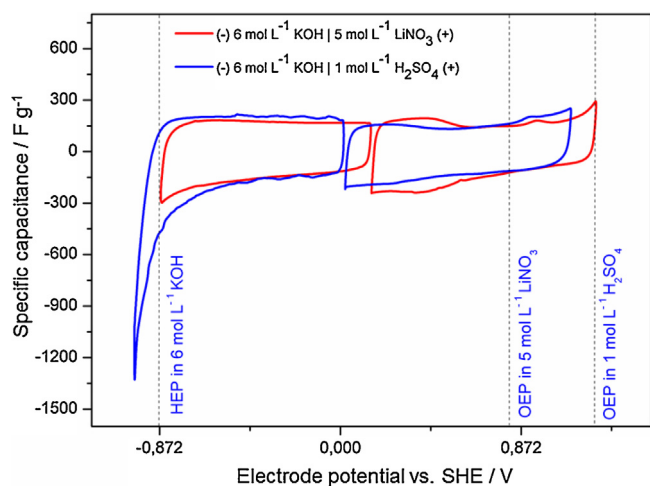


Fig. 6. Cyclic voltammograms for hybrid electrolyte capacitors in three electrode investigations, scan rate 5 mV s^{-1} . Hydrogen (HEP) and oxygen evolution potentials (OEP) are marked by dashed lines.

exceeds oxygen evolution potential (approaching the value of OEP in acidic medium). However, this response might be attributed to the local change of pH in the electrode bulk and is balanced by the negative electrode. That kind of electrochemical response allows the operational voltage of 2.1 V to be reached. A very similar situation was observed for second electrolyte combination, i.e. H_2SO_4 with KOH. The difference concerns the potentials of each electrode which are a little bit shifted to more negative values, i.e. ca. 120 mV. As a consequence, a peak on the cyclic voltammogram for the negative electrode corresponding to hydrogen evolution can be observed. For the positive electrode that operates in $1 \text{ mol L}^{-1} \text{H}_2\text{SO}_4$, OEP was not exceeded, so the CV profile resembles a quite rectangular shape.

Galvanostatic charging/discharging technique was applied in order to evaluate the capacitance retention at various regimes. These results were presented as the Ragone plot, to compare all investigated systems in respect of energy and power performance. One should note that the energy and power values have been calculated prior to the electrode mass (excluding casing, separator and mass of the electrolyte in the electrodes). The capacitance and energy values were estimated from iR-corrected discharge

branches. We are aware that the presented values do not consider a full device and thus might be overestimated, however, we believe that for comparison purpose, such Ragone plot perfectly illustrates a benefit of our concept.

Accordingly, from Fig. 7 one can notice a remarkable increase in energy density and relatively high power density enhancement

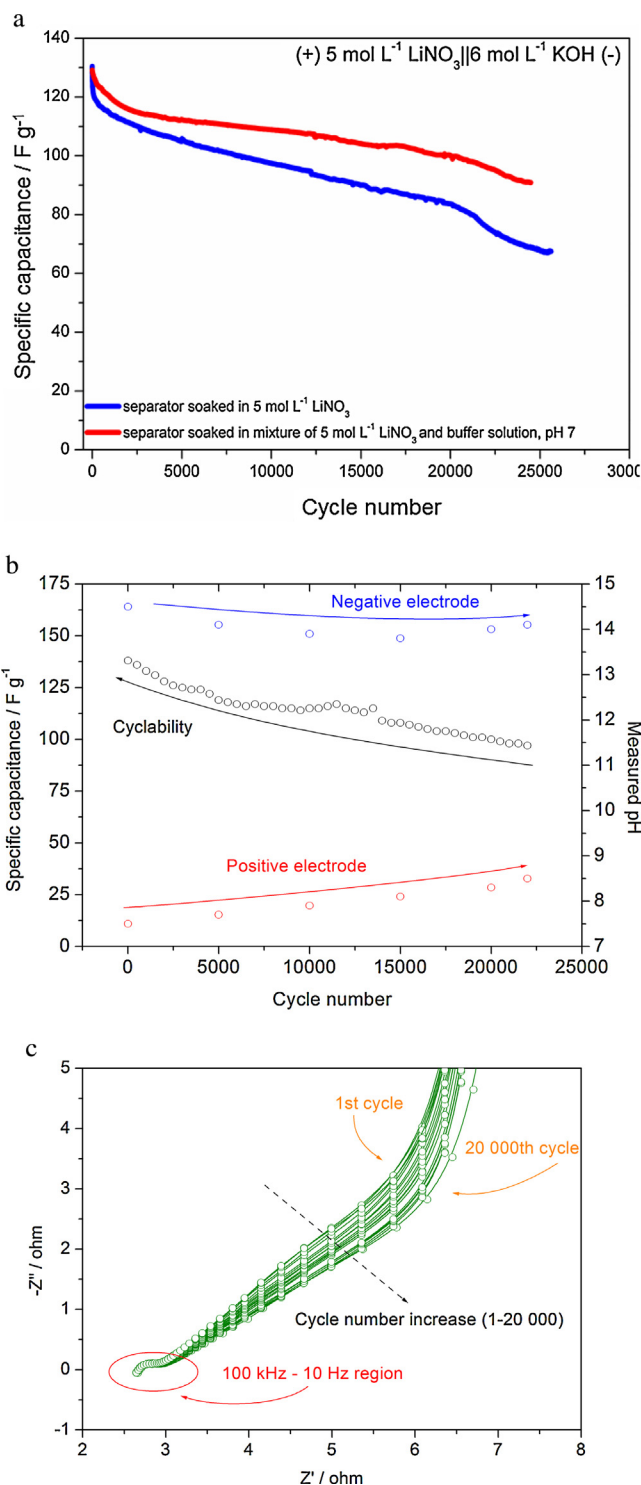


Fig. 8. (a) Capacitance vs. number of cycles dependence for neutral/alkaline capacitors with different separators and carbon tissue as electrode material (ACC 507-20). (b) pH changes of the electrolytes near to the electrodes for neutral/alkaline capacitor recorded during the cyclability measurement. (c) Nyquist diagrams (100 kHz–10 mHz) for neutral/alkaline capacitor recorded during the cyclability measurement (stepwise: 1000 cycles).

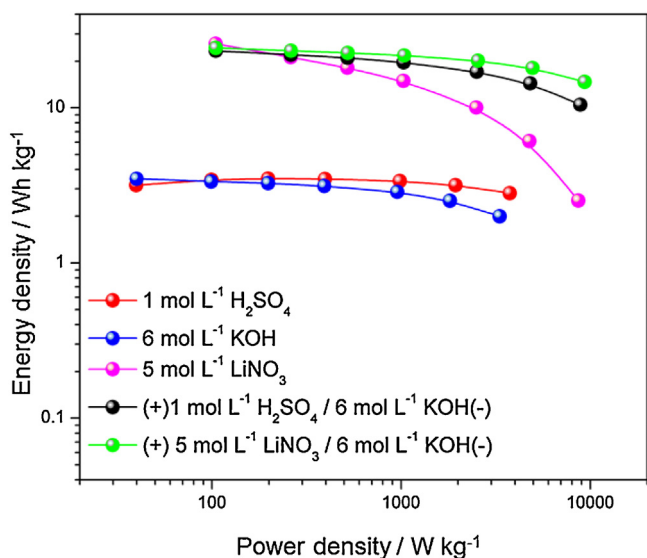


Fig. 7. Ragone plot for capacitors with different electrolytes.

when a couple of electrolytes is used. It provides an advantage over 'symmetric' H_2SO_4 and KOH solutions, which cannot operate at higher voltages. Moreover, even at a very high current load (20 A g^{-1}), the energy density is about 15 Wh kg^{-1} and maintains the power density of 10 kW kg^{-1} . For a single electrolyte much better results were demonstrated with device assembled with $5 \text{ mol L}^{-1} \text{ LiNO}_3$ because it can operate in voltage values up to 1.6 V . However, its performance is rather sensitive to higher current regimes. Thus, we can observe a significant capacitance fade, which is reflected by an energy density decay. At a current density of 20 A g^{-1} energy density decreases about 5 times comparing to presented hybrid solutions. Finally, we concluded that neutral/alkaline system has the optimal performance.

In order to determine cycling stability of the presented system galvanostatic charging/discharging technique was applied (1 A g^{-1}). Due to the fact that it is crucial to separate both electrolytes well, in order to maintain stable pH values near each electrode, two separator configurations were investigated. The separator was soaked in one of the following solutions: (1st) $5 \text{ mol L}^{-1} \text{ LiNO}_3$ (pH 7.7) aqueous solution, (2nd) a pure phosphate buffer solution (pH 7) and (3rd) $5 \text{ mol L}^{-1} \text{ LiNO}_3$ in phosphate buffer solution. The results are presented in Fig. 8a. In order to check the influence of buffer, we performed the cyclability with the separator soaked only in this solution (2nd option, not shown here), but the initial resistance and dramatic capacitance fade excluded this system from further investigations.

It can be seen that the highest capacitance with stable performance is maintained for the capacitor with the separator immersed in the mixture of lithium nitrate and buffer solution. Even if the capacitance decreases quite fast during the first 5 000 cycles (from 130 F g^{-1} to 112 F g^{-1}), after next 20 000 cycles the capacitance drop is only 20 F g^{-1} . As already mentioned, the worst performance was observed for the capacitor with the separator soaked in buffer solution. A sharp decrease of capacitance occurred in the first 500 cycles, which was probably caused by the faster mixing of electrolytes and pH change (confirmed by post-mortem study, with pH 13.9 on both sides). From this experiment, we concluded that a good separation of electrolytes is crucial and, furthermore, has been achieved by separating the electrodes by a buffer solution with LiNO_3 as ion carriers.

Additionally, we performed another cyclability tests for the optimal electrolyte combination i.e. (–)KOH/ LiNO_3 (+) separated with the glass fiber disc soaked in $5 \text{ mol L}^{-1} \text{ LiNO}_3$ in pH 7 buffer solution. During this study, pH of the electrolyte near to the

electrode surface was measured (Fig. 8b). It can be seen that pH of positive electrode electrolyte increased slightly from 7.5 to 8.5 whereas pH of negative electrode electrolyte was almost stable, with negligible variation around 14. It has to be noticed that for pH measurement, the capacitor was disassembled and then reassembled again. Hence, the cyclability seems to be a little bit worse than for non-open device.

Moreover, an impedance spectrum has been recorded after each 1 000 cycles within $100 \text{ kHz} - 10 \text{ mHz}$ range in order to observe the ESR changes (Fig. 8c). In high-frequency range, we did not observe any significant change or increase of ESR values. EDR seems to be stable as well, however, in the mid-frequency region, i.e. between 10 Hz and 1 Hz , more resistive behaviour has been observed. The slope of Nyquist profile approaching 45° angle suggests that the charge propagation is affected by transport (diffusion) phenomena. This is in good agreement with a pH change recorded; we assume that some part of OH^- ions population migrates throughout the separator which might aggravate the charge propagation.

In order to check the equilibrium state of the system, the self-discharge characteristic has been investigated. Both capacitors were charged with $+500 \text{ mA g}^{-1}$ current load to the expected voltage (1.8 V and 2.1 V for neutral/alkaline and acidic/alkaline systems, respectively) and afterwards no current was applied. The cut-off measurement conditions were as follows: either 6 hours of continuous self-discharge (without polarisation) or the voltage drop smaller than 1 mV h^{-1} . As presented in Fig. 9, the device with acidic/alkaline solution system has a significant self-discharge rate, i.e. 200 mV per time log-decade; in the case of a neutral/alkaline solution, this rate is remarkably smaller, i.e. 40 mV per time log-decade. Finally, after 6 hours, neutral/alkaline system reached 1.6 V of the cell voltage (12% of voltage drop) whereas acidic/alkaline system reached 1.1 V of the cell voltage (48% of voltage drop). The nature of such a self-discharge characteristic might be of various origin. However, the log scale self-discharge curve in both systems perfectly resembles linear behaviour. It suggests that the major contribution is related to the barrier of activation energy, i.e. contribution of possible faradaic reactions, charge re-distribution, parasitic corrosion processes, etc. The reorganization of ions at electrode/electrolyte interface towards equilibrium state should not be excluded too. At the same time, the self-discharge profiles suggest, that no typical redox phenomena (e.g. electrolyte decomposition) occur. Moreover, a pH change would provoke a faster self-discharge as the electrodes would tend to equilibrate

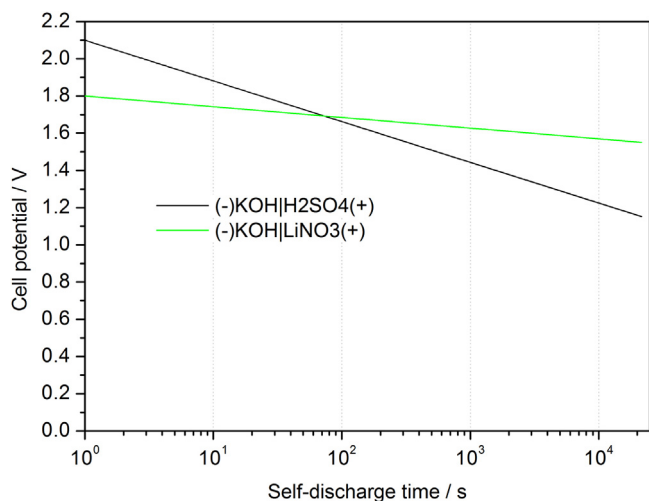


Fig. 9. Self-discharge profiles for capacitors operating in neutral/alkaline and acidic/alkaline combined electrolytes.

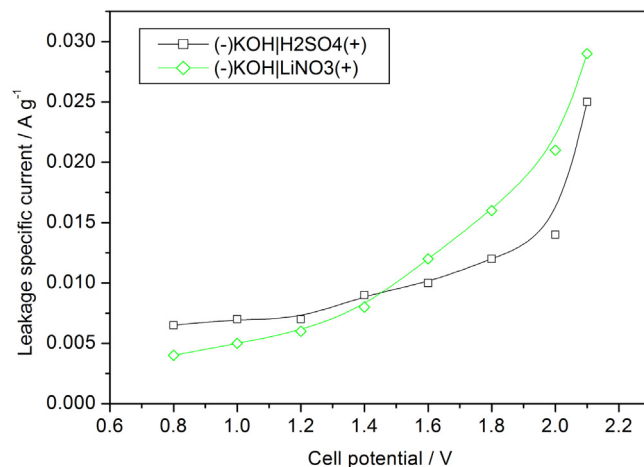


Fig. 10. Leakage current profiles for capacitors operating in neutral/alkaline and acidic/alkaline combined electrolytes.

their potentials prior to the surrounding medium. Finally, the ion transport related to OH^- or H_3O^+ flow would boost a self-discharge rate, and it would be observed as 'diffusion' (\sqrt{t}) not 'activation' ($\log t$)-dependent profile. For the moment, there is a small number of reports devoted to self-discharge mechanism [46], but authors do believe that self-discharge phenomenon indicates in fact that capacitor is in non-steady-state and tends to the thermodynamic equilibrium.

The leakage currents were measured during imposed potentiostatic polarisation at certain voltages in order to support the self-discharge investigations (see Fig. 10).

This measurement indicates that there is no direct correlation between self-discharge recorded; the leakage current densities were, in fact, higher for the neutral/alkaline system, whereas the self-discharge rate was higher for acidic/alkaline one. This suggests that leakage current is only one of the factors contributing to self-discharge phenomena. Moreover, it is accepted that leakage current measurement might indicate an optimal voltage for the system. Indeed, the inflection point (indicated by the second derivative of the curve) of the neutral/alkaline system is at 1.79 V while for acidic/alkaline at 1.98 V. A significant increase of leakage current measured might suggest other processes occurring in the system (either corrosion or electrolyte decomposition). It must be mentioned that these experiments were performed on laboratory constructed models (Swagelok cells), being quite far from real capacitor systems. Certainly, investigations carried out on coated electrodes with pouch cells (planned in the nearest future) would show more accurate results.

The final issue concerns the pH maintenance during long-term operation. This reasonable question arises when there is no specially designed membrane in the system to separate the solution with various pH; however, one should again notice that a) there is no excess of electrolyte solution, b) the separator has been soaked by buffering solution c) for the optimal assembly (neutral/alkaline), the difference in the concentration ($5 \text{ mol L}^{-1} \text{ LiNO}_3$ vs. $6 \text{ mol L}^{-1} \text{ KOH}$) and ionic strength is not as remarkable as in case of $6 \text{ mol L}^{-1} \text{ KOH}$ and $1 \text{ mol L}^{-1} \text{ H}_2\text{SO}_4$ (KOH solution has twice higher ionic strength). Hence, one can assume that transport throughout the separator is not very quick and preserves the stable pH in the electrode bulk. In order to evaluate the pH changes, the pH of the solution in the closest area of the electrode from the current collector side was measured using flat-membrane electrode. The results have been presented in Fig. 11.

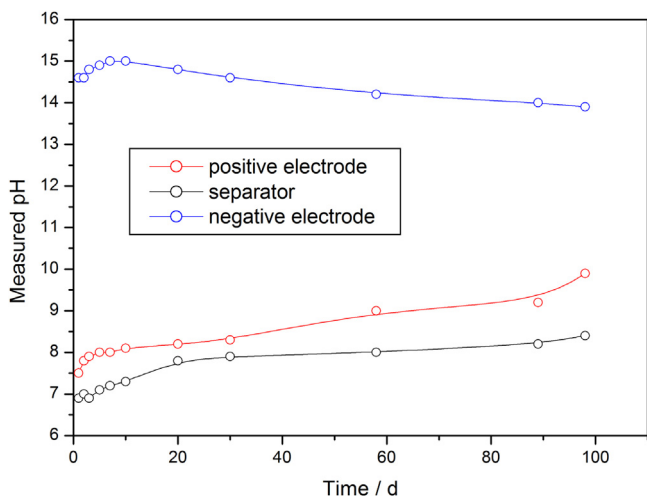


Fig. 11. pH variation along the shelf-life time of the solutions in neutral/alkaline capacitor; no voltage applied during storage.

One may note that pH varies with the time. However, the change is rather negligible. In the case of an alkaline solution, the pH oscillates around 1 pH unit while an increase of 2 pH units was observed for a neutral solution. The pH of the buffered separator solution is rather stable, but it seems that after time the buffering capacity has been almost reached. However, these measurements suggest that pH appears to be acceptably stable, at least, up to 100 days.

Authors are aware that the up-scale technological concept might be somewhat difficult, and several improvements are necessary. Nevertheless, the major goal of this study was to verify the idea grown on thermodynamic considerations. We do believe that first principles are of the greatest importance, and there is no discussion of their validity; finally, this work seems to be a great proof of that finding.

4. Conclusions

We demonstrated that the voltage of the capacitor with aqueous electrolyte does not have to be limited to 1.23 V. By introducing two electrolytes with different pH for each electrode we were able to obtain one system characterized by a very high potential of oxygen evolution and very low potential of hydrogen evolution. Therefore, it was possible to increase the capacitor voltage up to 2.1 V without remarkable electrolyte decomposition. Hence, such features of the aqueous capacitor as energy and power has been improved. In the case of neutral/base capacitor where its separator was immersed in mixture of $5 \text{ mol L}^{-1} \text{ LiNO}_3$ and a buffer solution (pH 7) it was possible to maintain almost 100 F g^{-1} after 25000 cycles at 1 A g^{-1} , giving the energy more than 10 Wh kg^{-1} along the average power of 1 kW kg^{-1} . However, the system is quite sensitive to pH change and requires cautious assembly. In this term, further investigations with other salts and types of electrolytes seem to be necessary.

Acknowledgements

The authors are grateful to the grant LIDER/018/513/L-4/12/NCBR/2013 funded by National Centre for Research and Development and Swiss Contribution of PSPB 107/2010 INGE project for financial support.

References

- [1] R. Kötzt, M. Carlen, Principles and applications of electrochemical capacitors, *Electrochim. Acta* 45 (2000) 2483–2498.
- [2] M.D. Levi, G. Salitra, N. Levy, D. Aurbach, J. Maier, Application of a quartz-crystal microbalance to measure ionic fluxes in microporous carbons for energy storage, *Nat. Mater.* 8 (2009) 872–875.
- [3] F.C. Wu, R.L. Tseng, C.C. Hu, C.C. Wang, Effects of pore structure and electrolyte on the capacitive characteristics of steam- and KOH-activated carbons for supercapacitors, *J. Power Sources* 144 (2005) 302–309.
- [4] F.C. Wu, R.L. Tseng, C.C. Hu, C.C. Wang, The capacitive characteristics of activated carbons-comparisons of the activation methods on the pore structure and effects of the pore structure and electrolyte on the capacitive performance, *J. Power Sources* 159 (2006) 1532–1542.
- [5] J. Huang, B.G. Sumpter, V. Meunier, Theoretical model for nanoporous carbon supercapacitors, *Angew. Chem. Int. Ed.* 47 (2008) 520–524.
- [6] D.W. Kirk, J.W. Graydon, Electrochemical double layer capacitance in activated carbon: Ion size effects, *ECS Trans.* 25 (2010) 163–171.
- [7] F. Béguin, V. Presser, A. Balducci, E. Frackowiak, Carbons and electrolytes for advanced supercapacitors, *Adv. Mater.* 26 (2014) 2219–2251.
- [8] A.B. Fuertes, G. Lota, T.A. Centeno, E. Frackowiak, Templated mesoporous carbons for supercapacitor application, *Electrochim. Acta* 50 (2005) 2799–2805.
- [9] C.O. Ania, V. Khomenko, E. Raymundo-Piñero, J.B. Parra, F. Béguin, *Adv. Funct. Mater.* 17 (2007) 828–836.
- [10] J. Eskusson, A. Jänes, A. Kikas, L. Matisen, E. Lust, Physical and electrochemical characteristics of supercapacitors based on carbide derived carbon electrodes in aqueous electrolytes, *J. Power Sourc.* 196 (2011) 4109–4116.
- [11] V. Presser, M. Heon, Y. Gogotsi, Carbide-derived carbons – from porous networks to nanotubes and graphene, *Adv. Funct. Mat.* 21 (2011) 810–833.

- [12] E.G. Bushueva, P.S. Galkin, A.V. Okotrub, L.G. Bulusheva, N.N. Gavrilov, V.L. Kuznetsov, S.I. Moiseev, Double layer supercapacitor properties of onion-like carbon materials, *Phys. Stat. Sol. (b)* 245 (2008) 2296–2299.
- [13] Y. Dall'Agnese, M.R. Lukatskaya, K.M. Cook, P.-L. Taberna, Y. Gogotsi, P. Simon, High capacitance of surface-modified 2D titanium carbide in acidic electrolyte, *Electrochem. Commun.* 48 (2014) 118–122.
- [14] M.D. Levi, M.R. Lukatskaya, S. Sigalov, M. Beidaghi, N. Shpigel, L. Daikhin, D. Aurbach, M.W. Barsoum, Y. Gogotsi, Solving the capacitive paradox of 2D MXene using Electrochemical Quartz-Crystal Admittance and In Situ Electronic Conductance measurements, *Adv. Energy Mater.* 5 (2015) 1400815.
- [15] Y. Shilina, M.D. Levi, V. Dargela, D. Aurbach, S. Zavorine, D. Nucciarone, M. Humeniuk, I.C. Halalay, Ion size to pore width ratio as a factor that determines the electrochemical stability window of activated carbon electrodes, *J. Electrochem. Soc.* 160 (2013) A629–A635.
- [16] J.P. Zheng, The limitations of energy density of battery/double-layer capacitor asymmetric cells, *J. Electrochem. Soc.* 150 (2003) A484–A492.
- [17] J.W. Long, D. Bélanger, T. Brousse, W. Sugimoto, M.B. Sassin, O. Crosnier, Asymmetric electrochemical capacitors—Stretching the limits of aqueous electrolytes, *MRS Bulletin* 36 (2011) 513–522.
- [18] T. Brousse, D. Bélanger, J.W. Long, To Be or Not To Be Pseudocapacitive? *J. Electrochem. Soc.* 162 (2015) A5185–A5189.
- [19] M.F. Dupont, Scott W. Donne, Separating the faradaic and non-Faradaic contributions to the total capacitance for different manganese dioxide phases, *J. Electrochem. Soc.* 162 (2015) A5096–A5105.
- [20] L. Coustan, F. Favier, Microwave-Assisted Decoration of Carbon Substrates for Manganese Dioxide-Based Supercapacitors, *J. Electrochem. Soc.* 162 (2015) A5133–A5139.
- [21] G. Lota, E. Frackowiak, Striking capacitance of carbon/iodide interface, *Electrochem. Commun.* 11 (2009) 87–90.
- [22] K. Fic, M. Meller, E. Frackowiak, Strategies for enhancing the performance of carbon/carbon supercapacitors in aqueous electrolytes, *Electrochim. Acta* 128 (2014) 210–217.
- [23] Q. Abbas, P. Ratajczak, P. Babuchowska, A. Le Comte, D. Bélanger, T. Brousse, F. Béguin, Strategies to improve the performance of carbon/carbon capacitors in salt aqueous electrolytes, *J. Electrochem. Soc.* 162 (2015) A5148–A5157.
- [24] B. Akinwalemiwa, C. Peng, G.Z. Chen, Redox Electrolytes in Supercapacitors, *J. Electrochem. Soc.* 162 (2015) A5054–A5059.
- [25] R. Lin, P. Huang, J. Ségalini, C. Largeot, P.L. Taberna, J. Chmiola, Y. Gogotsi, P. Simon, Solvent effect on the ion adsorption from ionic liquid electrolyte into sub-nanometer carbon pores, *Electrochim. Acta* 54 (2009) 7025–7032.
- [26] E. Frackowiak, G. Lota, J. Pernak, Room-temperature phosphonium ionic liquids for supercapacitor application, *Appl. Phys. Lett.* 86 (2005) 164104.
- [27] R. Palm, H. Kurig, K. Tönurist, A. Jänes, E. Lust, Is the mixture of 1-ethyl-3-methylimidazolium tetrafluoroborate and 1-butyl-3-methylimidazolium tetrafluoroborate applicable as electrolyte in electrical double layer capacitors? *Electrochem. Commun.* 22 (2012) 203–206.
- [28] V. Ruiz, C. Blanco, E. Raymundo-Piñero, V. Khomenko, F. Béguin, R. Santamaría, Effects of thermal treatment of activated carbon on the electrochemical behaviour in supercapacitors, *Electrochim. Acta* 52 (2007) 4969–4973.
- [29] V. Ruiz, R. Santamaría, M. Granda, C. Blanco, Long-term cycling of carbon-based supercapacitors in aqueous media, *Electrochim. Acta* 54 (2009) 4481–4486.
- [30] Q. Abbas, P. Ratajczak, F. Béguin, Sodium molybdate – an additive of choice for enhancing the performance of AC/AC electrochemical capacitors in a salt aqueous electrolyte, *Faraday Discuss.* 172 (2014) 199–214.
- [31] C. Peng, S. Zhang, X. Zhou, G.Z. Chen, Unequalisation of electrode capacitances for enhanced energy capacity in asymmetrical supercapacitors, *Energy Environ. Sci.* 3 (2010) 1499–1502.
- [32] J.H. Chae, G.Z. Chen, 1.9V aqueous carbon-carbon supercapacitors with unequal electrode capacitances, *Electrochim. Acta* 86 (2012) 248–254.
- [33] T.H. Wu, C.T. Hsu, C.C. Hu, L.J. Hardwick, Important parameters affecting the cell voltage of aqueous electrical double-layer capacitors, *J. Power Sources* 242 (2013) 289–298.
- [34] T.H. Wu, C.T. Hsu, C.C. Hu, L.J. Hardwick, Criteria appointing the highest acceptable cell voltage of asymmetric supercapacitors, *Electrochem. Commun.* 27 (2013) 81–84.
- [35] V. Khomenko, E. Raymundo-Piñero, F. Béguin, A new type of high energy asymmetric capacitor with nanoporous carbon electrodes in aqueous electrolyte, *J. Power Sources* 195 (2010) 4234–4241.
- [36] K. Fic, G. Lota, M. Meller, E. Frackowiak, Novel insight into neutral medium as electrolyte for high-voltage supercapacitors, *Energy Environ. Sci.* 5 (2012) 5842–5850.
- [37] L. Demarconnay, E. Raymundo-Piñero, F. Béguin, A symmetric carbon/carbon supercapacitor operating at 1.6V by using a neutral aqueous solution, *Electrochem. Commun.* 12 (2010) 1275–1278.
- [38] M.P. Bichat, E. Raymundo-Piñero, F. Béguin, High voltage supercapacitor built with seaweed carbons in neutral aqueous electrolyte, *Carbon* 48 (2010) 4351–4361.
- [39] L. Deng, G. Zhang, L. Kang, Z. Lei, C. Liu, Z.H. Liu, Graphene/VO₂ hybrid material for high performance electrochemical capacitor, *Electrochim. Acta* 112 (2013) 448–457.
- [40] Q. Gao, L. Demarconnay, E. Raymundo-Piñero, F. Béguin, *Energy Environ. Sci.* 5 (2012) 9611–9617.
- [41] Q. Abbas, D. Pajak, E. Frackowiak, F. Béguin, Effect of binder on the performance of carbon/carbon symmetric capacitors in salt aqueous electrolyte, *Electrochim. Acta* 140 (2014) 132–138.
- [42] G. Lota, T.A. Centeno, E. Frackowiak, F. Stoeckli, Improvement of the structural and chemical properties of a commercial activated carbon for its application in electrochemical capacitors, *Electrochim. Acta* 53 (2008) 2210–2216.
- [43] K. Fic, M. Meller, E. Frackowiak, Interfacial redox phenomena for enhanced aqueous supercapacitors, *J. Electrochem. Soc.* 162 (2015) A5140–A5147.
- [44] J. Jagiello, J.P. Olivier, 2D-NLDFT adsorption models for carbon slit-shaped pores with surface energetical heterogeneity and geometrical corrugation, *Carbon* 55 (2013) 70–80.
- [45] J. Jagiello, J.P. Olivier, Carbon slit pore model incorporating surface energetical heterogeneity and geometrical corrugation, *Adsorption* 19 (2013) 777–783.
- [46] H.A. Andreas, Self-discharge in electrochemical capacitors: A perspective article, *J. Electrochem. Soc.* 162 (2015) A5047–A5053.